Immunity, Volume *39*

Supplemental Information

Anthracyclines Induce DNA Damage Response-Mediated Protection against Severe Sepsis

Nuno Figueiredo, Angelo Chora, Helena Raquel, Nadja Pejanovic, Pedro Pereira, Björn Hartleben, Ana Neves-Costa, Catarina Moita, Dora Pedroso, Andreia Pinto, Sofia Marques, Hafeez Faridi, Paulo Costa, Raffaella Gozzelino, Jimmy L. Zhao, Miguel P. Soares, Margarida Gama-Carvalho, Jennifer Martinez, Qingshuo Zhang, Gerd Döring, Markus Grompe, J. Pedro Simas, Tobias B. Huber, David Baltimore, Vineet Gupta, Douglas R. Green, João A. Ferreira and Luis F. Moita

Supplemental Inventory

Supplemental Figures

Figueiredo *et al*. Fig S1

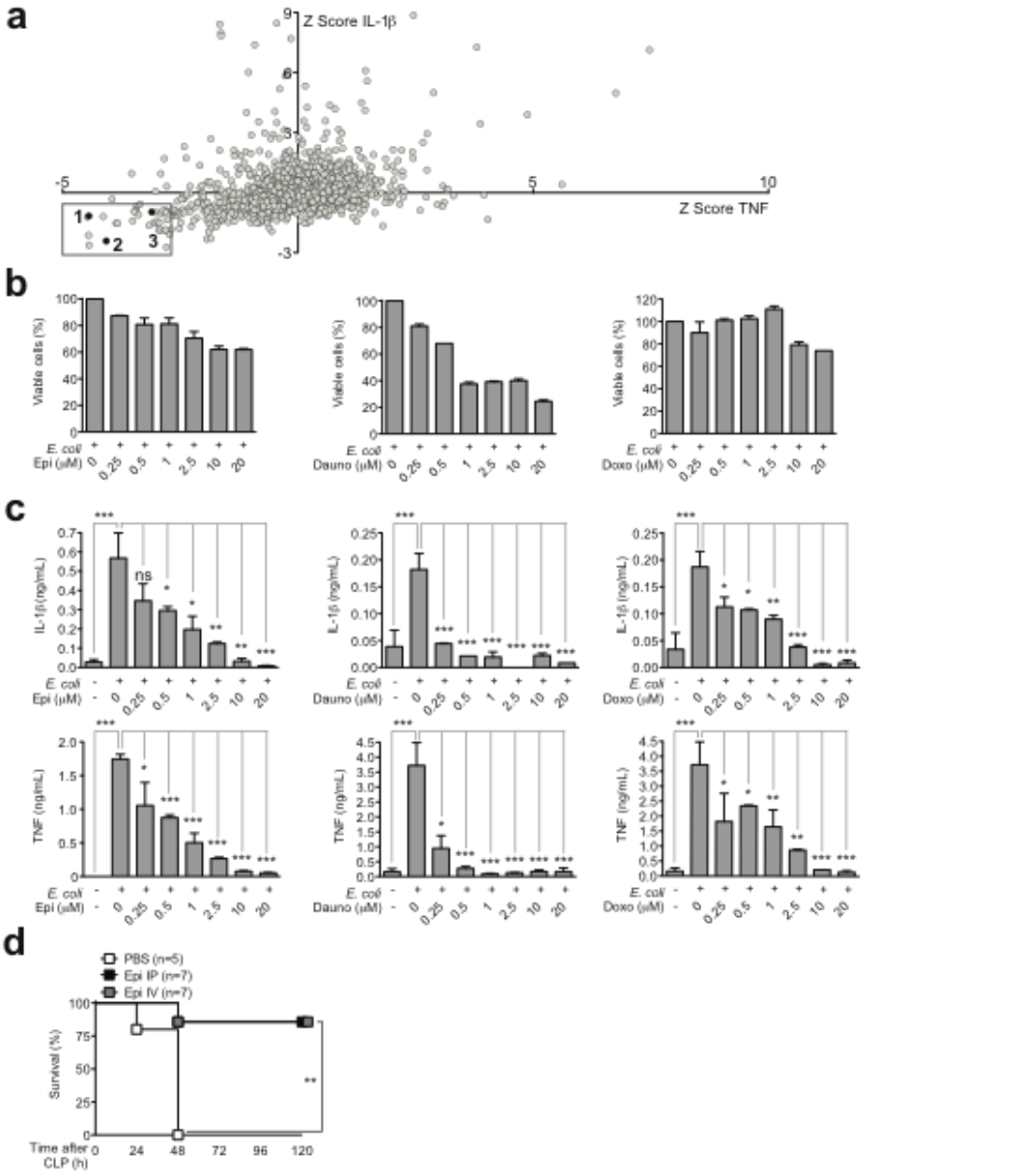

Figure S1 – Anthracyclines inhibit the secretion of TNF and IL-1β.
(a) Two-dimension plot of TNF and IL-1β production Z scores. The grey square defines the area in which compounds are considered primary hits, i.e., inhibiting both TNF and IL-1β. Black dots identify epirubicin (1), daunorubicin (2) and doxorubicin (3).
(b) THP-1 cell viability upon *E. coli* challenge (4 hours) after a pre-incubation (1 hour) with increasing concentrations of epirubicin (left panel), daunorubicin (middle panel) and doxorubicin (right panel).
(c) IL-1β and TNF production by *E. coli* challenged THP-1 cells (4 hours) after a pre-incubation (1 hour) with increasing concentrations of epirubicin (left panel), daunorubicin (middle panel) and doxorubicin (right panel).
(d) Survival of C57BL/6 wild-type animals subjected to CLP treated with carrier (PBS) or epirubicin (0.6µg/g body weight) intraperitoneally (Epi IP) or intraveneouslly (Epi IV) at the time of procedure and 24 hours later. Results shown represent arithmetic means ± SD from duplicate samples in one of 3 independent assays. ns, not significant; *P<0.05; **P<0.01 ***P<0.001 (Mann-Whitney test for (c); log-rank (Mantel-Cox) for (d)). Related to Figure 1.

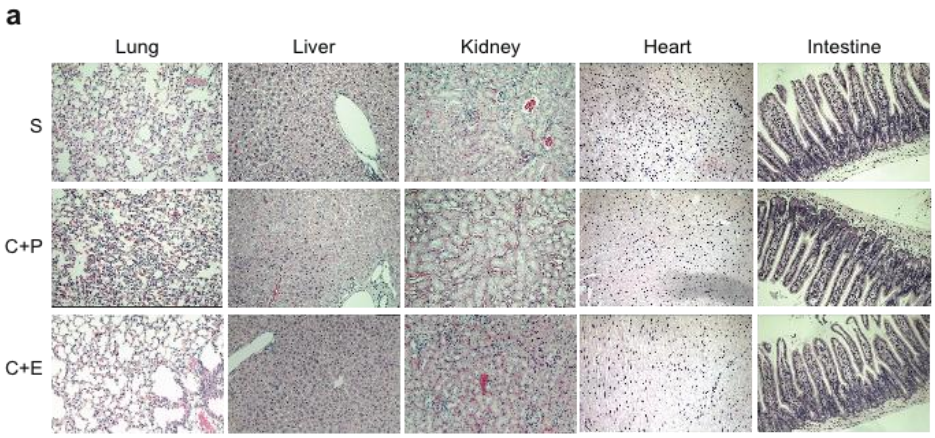

Figure S2 - Hematoxylin and eosin representative sections of lung, liver, kidney, heart and intestine of mice subjected to mock CLP (S) or CLP followed by treatment with PBS (C+P) or epirubicin (C+E) as in (a) and isolated 24 hours after the procedure. Original magnification 20X. Related to Figure 2.

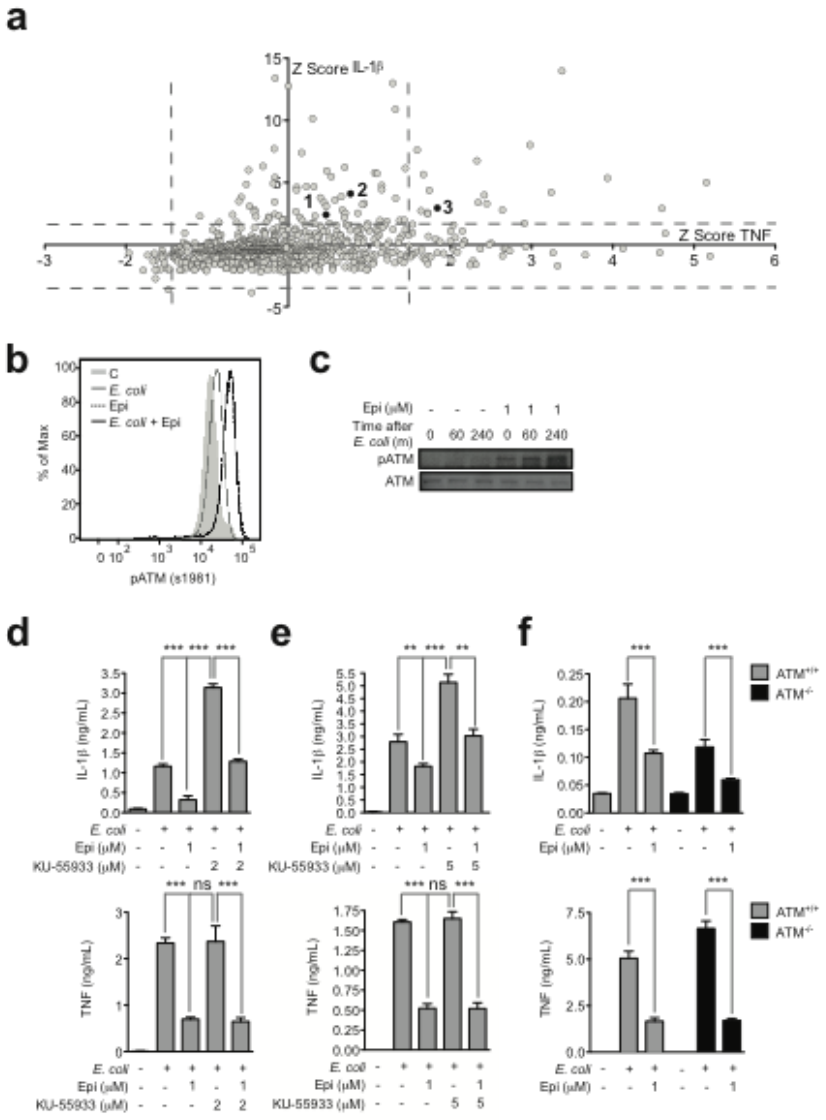
a
Z Score IL-1β
Z Score TNF
1
2
3
b
C
E. coli
Epi
E. coli + Epi
% of Max
pATM (s1981)
c
Epi (μM)
Time after E. coli (m)
0 60 240 0 60 240
pATM
ATM
d
IL-1β (ng/mL)
TNF (ng/mL)
E. coli
Epi (μM)
KU-55933 (μM)
ns
e
IL-1β (ng/mL)
TNF (ng/mL)
E. coli
Epi (μM)
KU-55933 (μM)
ns
f
IL-1β (ng/mL)
TNF (ng/mL)
ATM+/+
ATM-/-
E. coli
Epi (μM)

Figure S3 – The anti-inflammatory effects of epirubicin are mediated by ATM.
(a) Two-dimension Z score plot of TNF and IL-1β production by THP-1 cells upon target gene knockdown using a selected group of constructs of the TRC shRNA lentiviral vector library followed by PFA-fixed *E. coli* stimulation for 24 hours. Each dot represents an individual construct. Dotted horizontal and vertical lines define the area in which genes are considered primary hits. Black dots identify ATM (1), ATR (2) and CHECK1 (3).
(b) Epirubicin activates ATM as shown by Flow cytometry analysis of the activated form of ATM, phosphorilated at serine 1981, in THP-1 cells left untreated (C) or treated with epirubicin alone (1μM) (5 hours) (Epi), challenged with PFA-fixed *E. coli* (4 hours) (*E. coli*) or *E. coli* (4 hours) plus epirubicin pre-treatment (1 hour) (*E. coli* + Epi), and
(c) Immunoblotting of total protein extracts of THP-1 cells untreated or pre-treated with epirubicin (1mM) and challenged with PFA-fixed *E. coli* at indicated timepoints probed for the total and phosphorylated (serine 1981) forms of ATM.
(d) and **(e)** IL-1β and TNF production by (d) THP-1 cells and (e) BMDM following *E. coli* challenge (4 hours) after a pre-incubation (1 hour) with carrier, epirubicin or KU-55933 as indicated. Results shown represent arithmetic means ± SD from triplicate samples for one of at least 3 independent assays.
(f) IL-1β and TNF production by $Atm^{+/+}$ and $Atm^{-/-}$ BMDM following *E. coli* challenge and pre-incubation with carrier or epirubicin as in (e). ns, not significant; *P<0.05; **P<0.01 ***P<0.001 (Unpaired t test for (d) to (f)). Related to Figure 3.

Figueiredo *et al.* Fig S4

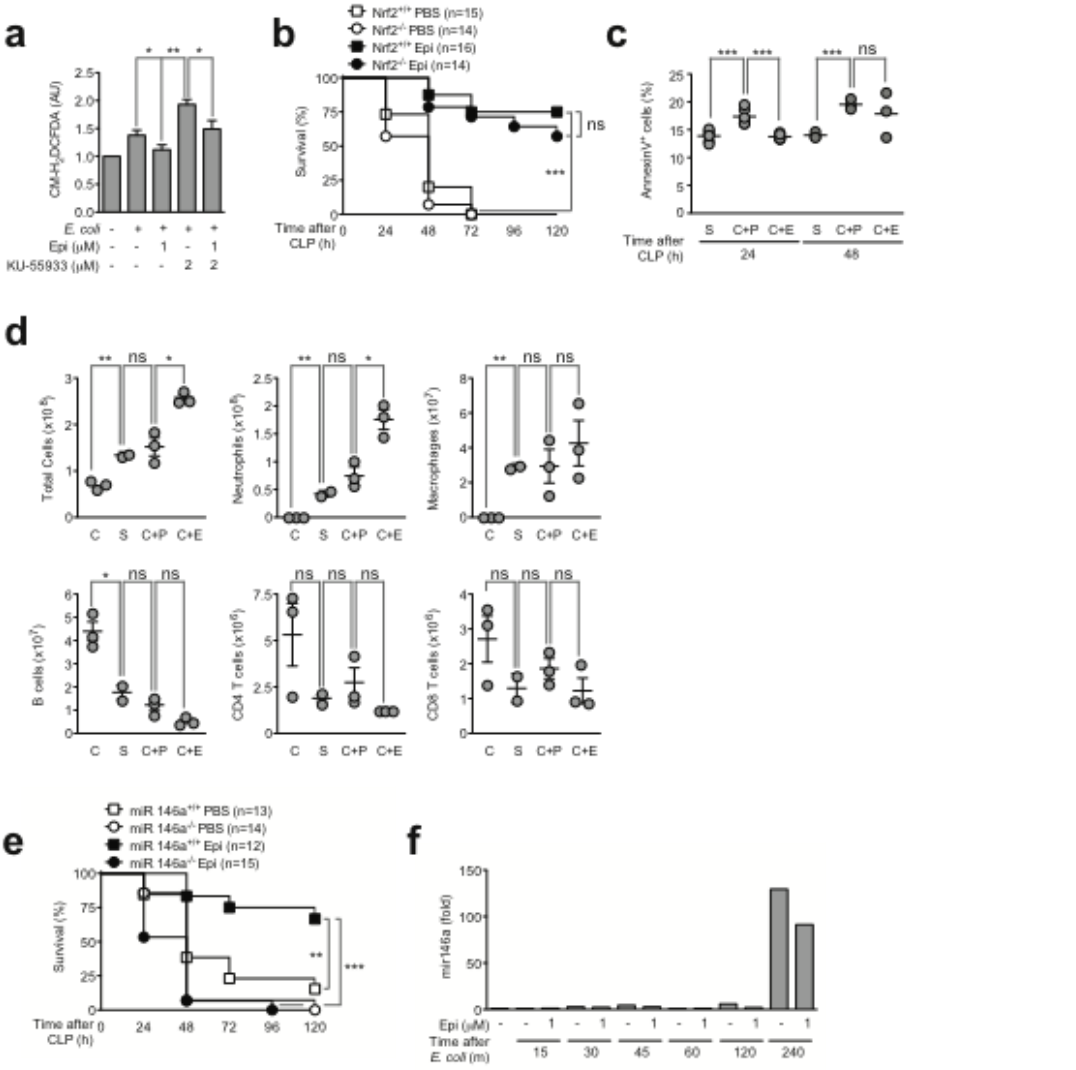

Figure S4 – In vivo protective effect of epirubicin is not due to either ROS scavenging, decreased neutrophils or induced miR-146a biogenesis.
(a) ROS content in THP-1 cells as assessed by the pan ROS probe CM-H_2DCFDA following *E. coli* challenge (4 hours) after a pre-incubation (1 hour) with carrier, epirubicin or KU-55933 as indicated. Results shown represent arithmetic means ± SEM from 3 independent assays.
(b) Survival of *Nrf2*$^{+/+}$ and *Nrf2*$^{-/-}$ animals subjected to CLP and treated with PBS or epirubicin (0.6µg/g body weight) (Epi) at the time of procedure and 24 hours later.
(c) Evaluation of apoptosis (AnnexinV^{+} cells) in total splenocytes of C57BL/6 wild-type animals subjected to CLP and treated with PBS or epirubicin as in (b) at the indicated times. Each circle represents individual animals and horizontal lines indicate arithmetic means ± SEM from two independent assays.
(d) Quantification of total cells, neutrophils, B cells, CD4 T and CD8 T lymphocytes in the peritoneal cavity 18 hours post CLP of C57BL/6 wildtype animals treated with PBS or epirubicin (0.6□g/g body weight) at the time of procedure.
(e) Survival of *miR 146a*$^{+/+}$ and *miR146a*$^{-/-}$ animals subjected to CLP and treated with PBS or epirubicin as in (b).
(f) *miR-146a* expression, as assessed by qRT-PCR, in THP-1 cells left untreated or pre-treated with epirubicin and challenged with PFA-fixed *E. coli* for the indicated times. ns, not significant; *P<0.05; **P<0.01; ***P<0.001 (unpaired t test for (a), (c) and (d); log-rank (Mantel-Cox) test for (b) and (e)). Related to Figure 4.

Figueiredo *et al.* Fig S5

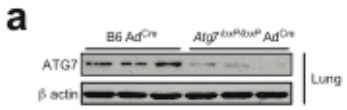

Figure S5 – Decreased expression of *Atg7* in the lung of *Atg7*$^{loxP/loxP}$ Ad^{Cre} animals.
(a) ATG7 protein levels by immunoblotting in lung of 3 wild-type (B6) and 3 *Atg7*$^{loxP/loxP}$ animals 5 days after inhalation of adenoviral vector encoding Cre (Ad^{Cre}). Related to Figure 5.

Supplemental Tables

ID	MOLECULE NAME	Z score TNFa	Z score IL1b
1505708	**EPIRUBICIN HYDROCHLORIDE**	**-4.474857631**	**-1.212875226**
300037	CRASSIN ACETATE	-4.448741528	-2.126298968
1501193	ERYSOLIN	-4.442389411	-1.162701697
1504079	TOMATINE	-4.440219344	-2.626087857
330001	DACTINOMYCIN	-4.13760156	-1.187827575
1505483	**DOXORUBICIN**	**-4.071115136**	**-2.412138965**
200007	GAMBOGIC ACID	-3.862359373	-1.529656531
200090	OBTUSAQUINONE	-3.829374842	-1.532189516
200022	AKLAVINE HYDROCHLORIDE	-3.511681732	-1.408917561
1504181	PRISTIMERIN	-3.474946679	-0.952562058
1505955	COLISTIN SULFATE	-3.457325884	-0.918619053
1504082	DIHYDROCELASTROL	-3.387513735	-1.102010407
1505908	MANGOSTIN TRIMETHYL ETHER	-3.162805301	-1.634164354
1504218	ACRISORCIN	-3.10607388	-0.959612692
300549	ACETYL ISOGAMBOGIC ACID	-3.056795183	-1.48116787
201522	GAMBOGIC ACID AMIDE	-3.013926221	-1.517154207
1500223	**DAUNORUBICIN**	**-3.007093086**	**-0.995459172**
201604	PYRROMYCIN	-2.980583694	-1.456377283
1500260	PYRITHIONE ZINC	-2.951809549	-1.872292546
201664	CELASTROL	-2.941287145	-1.499560887
1500319	GRAMICIDIN	-2.91855912	-1.84556962
1503006	BENZYL ISOTHIOCYANATE	-2.908582737	-1.034306584
1503904	PATULIN	-2.874616362	-0.902703858
1503640	PARTHENOLIDE	-2.842267433	-0.921962794
100005	ANTHOTHECOL	-2.834385142	-1.868706598
100009	CEDRELONE	-2.817231786	-1.852572153
1504098	PHENOTHRIN	-2.810792588	-0.982918754
1505438	HYDROCORTISONE VALERATE	-2.794271243	-2.722889618
1504240	1,4-NAPHTHOQUINONE	-2.77797604	-1.349015947
1505450	PREDNISOLONE HEMISUCCINATE	-2.72427413	-2.095888301
1500315	GENTIAN VIOLET	-2.696385799	-1.835724332
310010	HELENINE	-2.683894042	-0.943744357
310035	SANGUINARINE SULFATE	-2.651620816	-1.160017114
1503074	ALEXIDINE HYDROCHLORIDE	-2.648173863	-0.941221729
1503278	MITOXANTHRONE HYDROCHLORIDE	-2.562729474	-1.158920135
1505723	BETAMETHASONE ACETATE	-2.560814606	-0.950513609
100146	7-DESACETOXY-6,7-DEHYDROGEDUNIN	-2.517707805	-1.789647817
1503432	MEPARTRICIN	-2.504992413	-1.081865327
201524	DIHYDROGAMBOGIC ACID	-2.488781431	-1.48996453
1505722	DESOXYMETASONE	-2.417754689	-0.995122645
1505726	DESONIDE	-2.297715909	-0.945977097
1500521	PYRVINIUM PAMOATE	-2.268148981	-1.683811286
1505168	ETHACRIDINE LACTATE	-2.218841761	-1.389229184
1501149	RITODRINE HYDROCHLORIDE	-2.149761571	-1.268303571
1505125	ALCLOMETAZONE DIPROPIONATE	-1.999200408	-0.922964076

Supplemental Table S1 – List of drug candidates with a simultaneous effect on TNF and IL-1β secretion sorted according to the TNF score. Related to Figure 1.

GENE SYMBOL	Z score IL1b
RXRG	13.98549908
CERK	13.39528156
CDC2L2	12.99841134
CIB3	12.75588891
PINK1	10.89465184
MAP2K1IP1	10.14345798
SSH2	8.026894031
PANK4	7.718714959
EP300	7.623445834
AK7	7.394176161
NEK8	6.751890843
OBSCN	6.321377789
PKMYT1	6.226621005
HRAS	6.149535407
TRAF3IP3	6.002379966
NR1I3	5.95185992
MKNK1	5.779260808
LRRK1	5.719405322
RIPK2	5.660988701
GMIP	5.47911595
EGFR	5.412317129
GABRA3	5.359381956
TAF1	5.010952334
PGK2	4.917770486
PPP2R5A	4.857120549
UNK	4.771385393
GKAP1	4.683529402
TPD52L3	4.673580927
CNKSR3	4.618895483
INPP5D	4.438107961
ANP32A	4.395832296
ATPBD3	4.382323214
OTOF	4.208122584
ATR	4.112577436
CMPK	3.993795701
GABRA5	3.874921808
NR1H4	3.823781917
FASTK	3.778931417
UNK	3.732009689
ACVR1B	3.594003404
PFKP	3.491304822
NEK1	3.447427342
MYB	3.405296434
GLI2	3.384979498
LOC392265	3.321683768
PHKG2	3.302428028
CSNK1E	3.245684303
MGC16169	3.228807399

NRGN	3.095045302
PPP4R2	3.087946219
CHEK1	2.948032051
IKBKE	2.922117318
NRK	2.802732447
RET	2.790558375
NR1I2	2.789827176
PCK2	2.725958526
PIK3AP1	2.669418039
NF1	2.639991401
NME2	2.556120026
MAP3K11	2.534703827
RIMS4	2.5316375
UNK	2.478795985
KHK	2.438721798
ATM	2.416357404
IHPK3	2.415439713
RBL1	2.315787477
PRKCDBP	2.313302238
UNK	2.301598358
KRAS	2.272676173
PIK3CD	2.235319365
IGF1R	2.201867854
LOC442558	2.195176609
CDK5R1	2.105595811
MEN1	2.047194355

Supplemental Table S2 - shRNA-based identification of negative regulators of IL-1β secretion in response to *E. coli*, in THP-1 cells. Related to Figure 3.

Supplemental Experimental Procedures

Figure S1

Chemical Screen

THP-1 human monocytes were plated in 96-well plates at 10^6 cell/ml and incubated with each of the ~2320 compounds included in the Spectrum collection (Microsource Discovery Systems, Gaylordsville, CT) at 10μM for 1 hour. Cells were challenged with 4% PFA-fixed DH5a *E.coli* at a Multiplicity of Infection (MOI) of 20 bacterial cells per THP-1 cell for an additional 24 hours. The cell supernatants were collected and IL-1β and TNF cytokines quantified by DAS-ELISA, using Human IL-1β /IL-1F2 DuoSet® and Human TNF DuoSet® (R&D Systems®), respectively.

Figure S3

While epirubicin decreased both IL-1β and TNF secretion in THP-1 cells, only IL-1β, but not TNF, was up-regulated after ATM or ATR silencing (Supplemental Table S2 and S3). Similar results were obtained in THP-1 cells using the ATM specific pharmacologic inhibitor KU-55933 (Figure S3d). Similarly, treatment of bone marrow-derived macrophages with epirubicin inhibited IL-1β and TNF secretion (Figure S3e). However, this inhibition was also observed in ATM-deficient bone marrow derived macrophages, suggesting that epirubicin can inhibit IL-1β secretion via a mechanism that is not strictly ATM dependent (Figure S3f).

The RNAi Consortium Library

Detailed description of the RNAi Consortium (TRC) lentiviral RNAi library used in this study was originally described in (Moffat et al., 2006). More details can be found at www.broad.mit.edu/rnai/trc/lib.

shRNA-based Screen

We generated a working subset of The RNAi Consortium (TRC) shRNA lentiviral vector library (Moffat et al., 2006) that allows for the silencing of most of the genes that are either human kinases or phosphatases. This subset was composed of 1440 individually arrayed lentiviral shRNA vectors targeting ~700 genes, after selecting the most efficient shRNAs (two on average) based on available silencing efficiency data from the Broad Institute of MIT and Harvard. THP-1 cells were plated in 96-well plates at 10^6 cell/ml and infected with shRNA-expressing lentivirus. 48 hrs later infected cells were selected with puromycin. After the 3 days of selection, plates were duplicated. One of the plates was used to measure the cell number using Alamar Blue® cell viability assay (Invitrogen®). In the other plate, cells were stimulated with 4% PFA-fixed DH5a *E.coli* at a Multiplicity of Infection (MOI) of 20 bacterial cells per THP-1 cell. Twenty-four hours after stimulation, cell supernatants were collected and IL-1β and TNF cytokines quantified by DAS-ELISA. All data values from IL-1β and TNF secretion assays were normalized by dividing the amount of IL-1β and TNF in the conditioned media 24, 12, 8, 6, 4 or 2 hrs after *E. coli* stimulation by the number of cells in each well and then by the average concentration per cell of the plate. Results were logarithmic natural transformed. Scores were sorted in ascending order and graphed. We calculated 1.5 SDEVs above and below the mean to identify the genes that changed IL-1β and TNF secretion when silenced. The

same approach was used to identify the compounds that changed IL-1β and TNF secretion. The selected genes were submitted to two or more rounds of phenotypic validation.

Figure S4

We explored several additional possible ATM-dependent mechanisms to explain the protective role of epirubicin in sepsis. We found that, *in vitro,* epirubicin is able to counteract the increase in ROS generated by *E. coli* challenge of THP-1 cells in an ATM dependent manner (Figure S4a). However, mice that are deficient for the nuclear factor (erythroid-derived 2)-like 2 (NRF2), a master regulator of ROS scavenging (Lee et al., 2005), are still protected by epirubicin against mortality due to CLP (Figure S4b). Therefore, epirubicin induces an ATM-dependent ROS scavenging response that is largely dispensable for its protective effect in sepsis. Increased apoptosis of neutrophils can attenuate sepsis pathogenesis (Garrison et al., 2011). This would be a simple and attractive hypothesis considering that anthracyclines initiate a DDR leading to increased apoptosis if the DNA lesion is too severe for repair (Garrison et al., 2011). However, our data shows that epirubicin treated mice have higher, not lower, numbers of viable neutrophils in the abdomen, excluding an important role for this mechanism (Figure S4c).

The biogenesis of some miRNAs, including miR-146a (a negative regulator of inflammation (Taganov et al., 2007) and a proposed biomarker in sepsis (Wang et al., 2010)), is ATM-dependent (Zhang et al., 2011). We compared the survival of wild-type mice with that of miR-146a –deficient mice in the presence or absence of epirubicin. We conclude that the protection given by this drug is dependent on the presence of miR-146a (Figure S4e). However, our RT-qPCR analysis of miR-146a expression in either RAW cells or THP-1 cells (Figure S4f) does not support a role for epirubicin in the induction of this microRNA. Therefore, direct induction of miR- 146a is not the mechanism by which epirubicin protects against the LPS model of septic shock or CLP.

Supplemental References

Garrison, S.P., Thornton, J.A., Hacker, H., Webby, R., Rehg, J.E., Parganas, E., Zambetti, G.P., and Tuomanen, E.I. (2011). The p53-target gene puma drives neutrophil-mediated protection against lethal bacterial sepsis. PLoS Pathog *6*, e1001240.

Lee, J.M., Li, J., Johnson, D.A., Stein, T.D., Kraft, A.D., Calkins, M.J., Jakel, R.J., and Johnson, J.A. (2005). Nrf2, a multi-organ protector? FASEB J *19*, 1061-1066.

Moffat, J., Grueneberg, D.A., Yang, X., Kim, S.Y., Kloepfer, A.M., Hinkle, G., Piqani, B., Eisenhaure, T.M., Luo, B., Grenier, J.K., *et al.* (2006). A lentiviral RNAi library for human and mouse genes applied to an arrayed viral high-content screen. Cell *124*, 1283-1298.

Taganov, K.D., Boldin, M.P., and Baltimore, D. (2007). MicroRNAs and immunity: tiny players in a big field. Immunity *26*, 133-137.

Wang, J.F., Yu, M.L., Yu, G., Bian, J.J., Deng, X.M., Wan, X.J., and Zhu, K.M. (2010). Serum miR-146a and miR-223 as potential new biomarkers for sepsis. Biochem Biophys Res Commun *394*, 184-188.

Zhang, X., Wan, G., Berger, F.G., He, X., and Lu, X. (2011). The ATM kinase induces microRNA biogenesis in the DNA damage response. Mol Cell *41*, 371-383